Article (refereed) - postprint

Takriti, Mounir; Wynn, Peter M.; Elias, Dafydd M.O.; Ward, Susan E.; Oakley, Simon; McNamara, Niall P. 2021. **Mobile methane measurements: effects of instrument specifications on data interpretation, reproducibility, and isotopic precision.**

1 **Mobile methane measurements: Effects of instrument**

2 **specifications on data interpretation, reproducibility,**

3 **and isotopic precision**

4 Takriti, Mounir[a], Wynn, Peter M.[a], Elias, Dafydd[b], Ward, Susan E.[a],

5 Oakley, Simon[b] McNamara, Niall P.[b]

6

7 [a]Lancaster Environment Centre, Lancaster University, Bailrigg, Lancaster, LA1 4YQ, UK

8 [b]UK Centre for Ecology and Hydrology, Lancaster Environment Centre, Library Avenue,

9 Bailrigg, Lancaster, LA1 4AP, UK

10

12

13

14

15

Abstract

Recent research has used mobile methane (CH_4) measurements to identify and quantify emissions, but the effect of instrument response time on concentration measurements is rarely considered. Furthermore, stable isotope ratios are increasingly used in mobile measurements to attribute sources, but the precision of mobile isotopic measurements depend on a combination of instrument and measurement conditions. Here we tested the effect of instrument speed on concentration measurements by outfitting a vehicle with isotopic and concentration-only gas analysers with different response times and conducting multiple mobile surveys. Additionally, we performed a sensitivity analysis for the isotopic precision achievable under different conditions by programming a physical model, validated with empirical data from our mobile surveys. We found that slower response time led to a greater underestimation of measured CH_4 concentration, during both driving and stationary measurements, while the area under peaks in concentration is consistent and provides a robust means of comparing data between instruments. We also explore the use of an algorithm to improve instrument response. Our sensitivity analysis showed that the precision of isotopic measurements increases with the concentration range and the duration of the measurement following a power law. Our findings have important implications for the reporting and comparability of results between surveys with different instrumental setups and provide a framework for optimising sampling strategies under given objectives, conditions, and instrument capabilities.

1. Introduction

Atmospheric concentrations of methane (CH_4) have increased by more than 160 % since pre-industrial times and continue to rise. As CH_4 has 32 times the global warming potential of CO_2 (Etminan et al., 2016), there has been increasing focus on reducing emissions from anthropogenic sources, such as natural gas infrastructure, agriculture, and waste treatment. However, efforts to reduce emissions are still hampered by uncertainty around the location and contribution of different fugitive emission sources, and there is often considerable

44 disagreement between inventory estimates and atmospheric measurements (e.g. Turner et

45 al., 2016).

46 Vehicle mounted mobile measurement systems, which use gas analysers based on infrared

47 absorption spectroscopy, were used as early as the 1990s to quantify landfill CH_4 emissions

48 (Czepiel et al., 1996). More recent advances in spectroscopic gas analysers have led to the

49 increasing use of mobile systems to map CH_4 concentrations, detect fugitive emission sources,

50 and quantify emission rates (e.g. Fischer et al., 2017; Jackson et al., 2014). The origin of

51 emissions can be ambiguous, particularly if there are multiple emission sources in an area.

52 Using analysers that measure CH_4 concentrations and $^{13}CH_4$ isotope ratios can help distinguish

53 between emission sources. In particular, it becomes possible to distinguish between microbial

54 sources, such as landfills or agricultural emissions, which are typically depleted in $^{13}CH_4$, and

55 thermogenic sources, such as natural gas extraction and distribution, which are typically

56 enriched in $^{13}CH_4$.

57 While mobile CH_4 measurements do not provide continuous data over time and roadway

58 measured concentrations can strongly depend on meteorological conditions, they offer

59 several advantages compared to point measurements or lab analysis of field samples: 1) High

60 spatial resolution as CH_4 concentration can be mapped at a scale of meters; 2) good spatial

61 coverage as, depending on road access, tens to hundreds of kilometres can be covered within

62 days; 3) immediate detection of elevated concentrations enabling rapid investigation, e.g.

63 response to gas leaks. This approach therefore offers wide applications within academic

64 research, industry monitoring and maintenance, as well as regulatory oversight and

65 compliance monitoring.

66 Instrument manufacturers have been developing systems that integrate sampling, gas

67 analysis, navigation, and data processing, marketed primarily as turn-key solutions for leak

68 detection in the natural gas industry. Both pre-built systems and user-built set-ups have been

69 used for a variety of applications: tracer release studies to quantify emissions from waste

70 water treatment plants (Yoshida et al., 2014) and landfills (Mønster et al., 2014); measuring

71 fence line CH_4 and H_2S at gas wells (Eapi et al., 2014); attributing oil and gas emissions using

72 $^{13}CH_4$ and C_2H_6 measurements; mapping urban gas pipeline leaks (Jackson et al., 2014) and

73 estimating leak rates (Fischer et al., 2017); and assessing emissions from geological fault lines

74　(Boothroyd et al., 2016). The use of mobile survey systems may therefore increase in the

75　future as spectroscopic gas analysers become more widely available, and new applications,

76　such as operation on unmanned aerial vehicles, are explored (Allen et al., 2019). However,

77　the published literature on mobile CH_4 measurements has mainly focussed on the

78　dissemination of results, and while instrument setup and performance have been described

79　in detail elsewhere (e.g. Rella et al., 2015a), the effects of instrument specifications on results

80　obtained and their interpretation have rarely been discussed.

81　The range of instrumental setups used in mobile monitoring systems is increasing, and

82　applications are moving from one-off surveying campaigns to routine monitoring of regional

83　fugitive emissions (Albertson et al., 2016). It is thus essential to consider how hardware

84　specifications will affect performance and suitability for different applications, particularly

85　with regards to reproducibility and comparability of data.

86　Current mobile spectroscopic gas analysers, such as used in this study, measure

87　concentrations with precisions in the ppb range. While this level of precision is generally

88　sufficient for the requirements of mobile surveys, measured concentrations are not

89　necessarily equal to atmospheric concentrations, due to a lag in instrument response.

90　The response time of an instrument consists of two components: the transit time and the rise

91　time. Transit time is the time required for a volume of air to move from the air inlet to the

92　analyser cavity. This can easily be corrected for when matching concentration and location

93　data, and does not affect the measured concentration as such, although diffusive mixing of

94　air in the sampling system will increase with increasing tube volume and decreasing flow rate.

95　The rise time is the time delay between an initial step change in gas concentration and the

96　response in measured concentration of the analyser. It reflects the change in gas composition

97　in the analyser cavity as the gas is replaced continuously while the instrument goes through

98　measurement cycles, and is typically given as T_{90}, the time it takes for the measured

99　concentration to reach 90% of the final concentration. When a step change in concentration

100　occurs, the final concentration is only measured if it is sampled for the duration of the rise (or

101　corresponding fall) time (Brunner and Westenskow, 1988). This can lead to underestimation

102　of atmospheric concentrations in mobile measurements and impede comparability of results

103   obtained with different instrumental setups. The effect of rise time on gas concentration

104   measurements has been previously explored for respiration measurements in clinical settings

105   (Brunner and Westenskow, 1988; Schena et al., 1984; Tang et al., 2005) where mathematical

106   corrections have been developed to improve instrument response (Arieli and Van Liew, 1981;

107   Farmery and Hahn, 2000).

108   Additional considerations apply when using isotopic gas analysers to distinguish between

109   emission sources: current mobile spectroscopic gas analysers measure $^{13}CH_4/^{12}CH_4$ ratios with

110   two orders of magnitude lower precision than isotope ratio mass spectrometry (IRMS)

111   systems (Zazzeri et al., 2015). Moreover, instrument precision is generally specified for

112   averages of continuous measurements of a sample over a period of time, while mobile

113   measurements are variable and typically use regression analysis, such as with Keeling or

114   Miller-Tans plots, to derive source isotope signature estimates (e.g. Lopez et al., 2017; Rella

115   et al., 2015a). The effective precision during mobile measurements thus depends on a variety

116   of factors, including both instrument and emission characteristics.

117   Here, to investigate the effects of instrument response time on different measures of CH_4

118   emissions and their comparability between instruments, we compare concentration data

119   produced by two different instruments using a custom-built mobile system built around an

120   isotopic ($^{13}C/^{12}C$) CH_4 gas analyser, and a concentration-only CH_4 gas analyser. Additionally,

121   we perform a sensitivity analysis using Monte Carlo simulations of a simple physical model to

122   quantify the effects of instrument parameters and sampling conditions on the isotopic

123   precision of mobile measurements. The model results were validated by comparing our

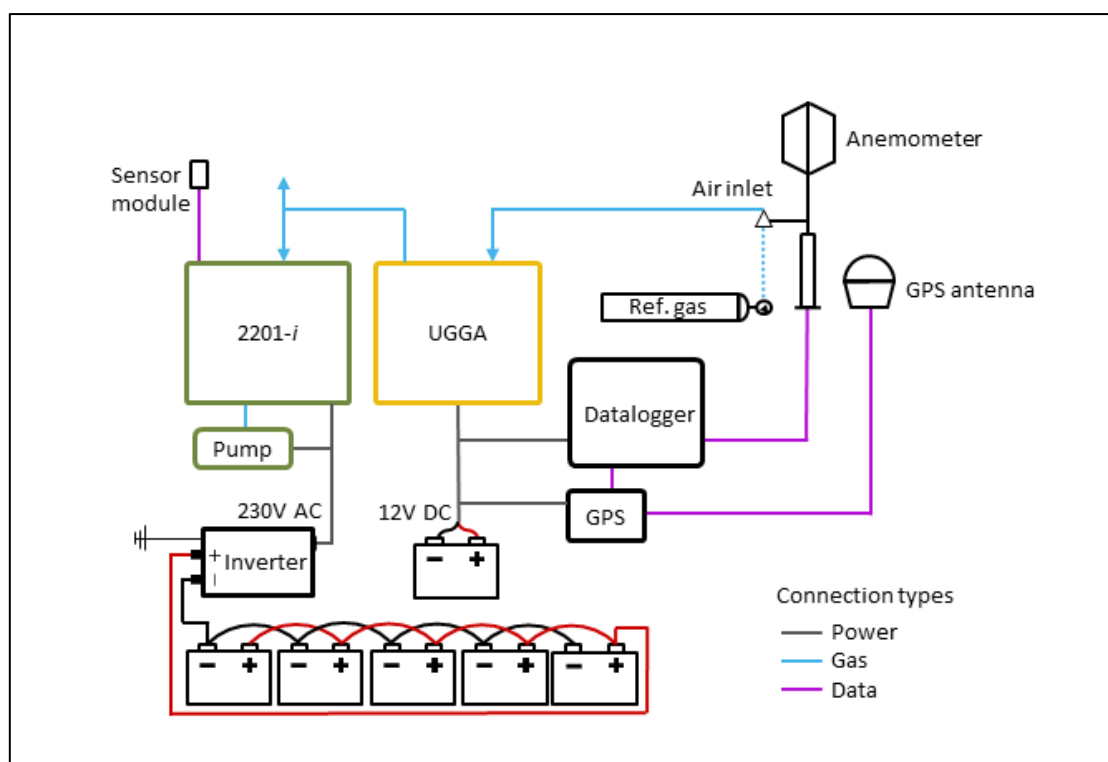124   empirical estimates of source signature precision with outputs of model simulations.

125   2. Materials and methods

126   2.1. Methane measurements

127   To evaluate the effect of instrument response time on CH_4 measurements in the field, a

128   vehicle (Mitsubishi L200) was equipped with two gas analysers, a Picarro G2201-*i* isotopic gas

129   analyser (Picarro Inc. Santa Clara, USA) and a Los Gatos Research Ultraportable Greenhouse

130   Gas Analyzer (Los Gatos Research Inc., San Jose, USA), henceforth referred to as G2201-*i* and

131   UGGA, respectively.

132 The G2201-*i* and the UGGA have a measurement frequency of 0.26 Hz and 1.2 Hz, and flow

133 rates of 25 mL min^{-1} and 650 mL min^{-1}, respectively. The rise time, i.e. the time to reach 90%

134 of the final concentration measurement in response to a step change in concentration (T_{90}) is

135 38 s for the G2201-*i* and 14 s for the UGGA. Both instruments measure CO_2, CH_4, and H_2O

136 concentrations in air. The instrument specifications differ largely because they are optimized

137 for different tasks and capabilities: the G2201-*i*'s lower flow rate enables more precise isotope

138 measurements, whereas the UGGA is designed for applications that require a rapid response

139 to concentration changes, such as flux measurements.

140 The air inlet was attached to the pole of the anemometer (see below) on the roof of the

141 vehicle, with the opening facing downward and terminating in a cone to prevent water

142 ingress. This air inlet was connected to the air inlet of the UGGA via a 310 cm nylon tube with

143 an outer/inner diameter of 6 mm/3 mm. A PTFE air filter (Vacushield, Pall Life Sciences, MI,

144 USA) was mounted on the inlet and airflow could be redirected via a solenoid valve to a drying

145 column inside the vehicle during instrument shutdown or to protect the instrument from

146 moisture intake. The two gas analysers were connected in series with the G2201-*i* air inlet

147 connected to the UGGA air outlet (Figure 1). Excess air flow was vented via an open split. The

148 output of each analyser was broadcast via Wi-Fi to two tablet devices mounted in front of the

149 passenger seat so that measurements could be monitored in real time. The G2201-*i* was

150 powered by five 72 Ah deep cycle batteries connected in parallel to a pure sine wave power

151 inverter, other components used DC power from a single battery (Figure 1). All components

152 were mounted on a wooden frame, with compartments for instruments and batteries, that

153 was secured on the bed of the vehicle. The batteries provided enough charge to operate the

154 system for over 10 h of continuous measurements. For electrical safety, fuses were installed

155 between the batteries and the power inverter, as well as in the DC circuit. The AC system was

156 grounded to the chassis of the vehicle.

Figure 1 Schematic of mobile system built around a Picarro 2201-*i* isotopic gas analyser and a Los Gatos Research UGGA gas analyser. GPS is a Hemisphere R330 differential GPS, anemometer is a WindMaster PRO 3-Axis Ultrasonic Anemometer, sensor module contains an accelerometer and environmental sensors. Dotted line shows a temporary connection between the reference gas cylinder and the air inlet only used during drift checks.

2.2. Location and wind data

Location and speed were measured by a R330 GNSS Receiver with a Hemisphere A21 Antenna (Hemisphere GNSS Inc., Arizona, USA) mounted on the vehicle roof providing location data with a nominal accuracy of ≤ 0.5 m. Wind speed and direction were measured using a roof mounted WindMaster PRO 3-Axis Ultrasonic Anemometer (Gill Instruments Ltd. Hampshire, UK). Data from both instruments were recorded to a CR6 datalogger (Campbell Scientific, Loughborough, UK) at 10 Hz and calculations were made in post processing, see SI.

2.3. Laboratory testing

The transit time between the air inlet and the gas analysers was measured by connecting two reference gases to the air inlet via a three-way valve and measuring the delay in the change in concentration when switching from one reference gas to another. Gas passing through an instrument's cavity may be mixed and therefore affect subsequent measurements at the
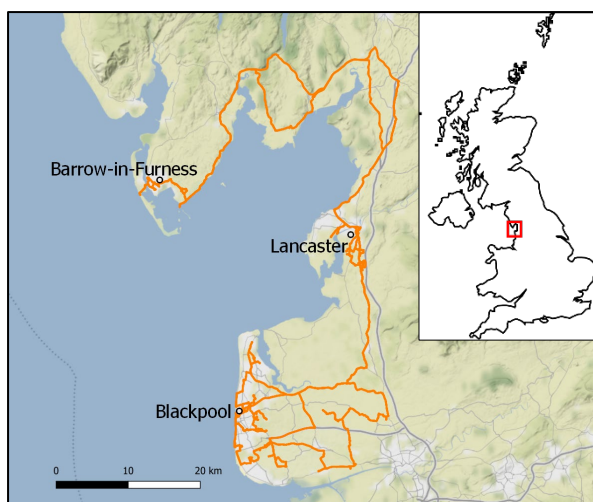
175   outlet. To test if setting up the two gas analysers in series would affect measurements made

176   by the G2201-*i*, standards with 3.03 ppm CH_4 and 10.1 ppm CH_4 were run through either just

177   the G2201-*i* or both instruments, connected in series for 10, 30, 60, and 120 seconds. No

178   significant differences in peak height, peak width, and peak area were found (paired t-test, n

179   = 3, p-values > 0.3).

2.4. Standard calibration and drift check

181   Before surveys, the gas analysers were calibrated for concentration using certified standards

182   with concentration of 3.03 ppm CH_4 and 10.4 ppm CH_4 (BOC Ltd., Guildford, UK) introduced

183   through the system's air inlet. The G2201-*i* was calibrated for $\delta^{13}CH_4$ using isotopic standards

184   with -23.9 ‰, -54.5 ‰, and -66.5 ‰ (Isometric Instruments, Victoria, Canada), covering the

185   range of expected isotope ratios in the study area. Calibration standards were measured for

186   10 minutes each. To check for instrument drift during mobile surveys, a reference gas cylinder

187   was mounted in the vehicle and gas was run through the sampling system immediately

188   before, during, and after sampling campaigns for 10 minutes each. For individual sampling

189   days, the standard deviations for mean CH_4 concentration measurements were 4 ppb for the

190   UGGA and 0.9 ppb for the G2201-*i*, on average. Mean precision of $\delta^{13}CH_4$ measurements for

191   individual sampling days was 0.73 ‰. Across all four sampling days, standard deviations were

192   14 ppb and 13 ppb, respectively, and precision was 0.74 ‰.

2.5. Field data collection

194   Field data were collected between November 2016 and March 2017 in the Fylde and

195   Morecambe Bay areas in Lancashire and Cumbria, North West England, UK (54°00'N., 2°48'W,

196   Figure 1). The area includes farmland, landfills, coastal wetlands, and natural gas processing

197   and distribution infrastructure, and therefore a range of both biogenic and thermogenic

198   emission sources. A total of 557 km was driven at a mean speed of 42 km h^{-1}. When

199   encountering notably elevated CH_4 concentrations, the vehicle was stopped downwind for ~

200   10 minutes, traffic conditions permitting, to improve precision of isotopic measurements.

201

Figure 2 Overview of study area and route of surveys. Map insert shows location of study area within the UK.

2.6. Data analysis

2.6.1. Methane concentration analysis

For mobile surveys, what measurements count as an elevated concentration, or peak, has to be defined. The simplest approach is to use a fixed threshold and to define measurements above the threshold as peaks. However, background concentrations can vary between different areas and measurement times. Moving averages can therefore be more suitable unless a very conservative threshold is used. For example, Fischer et al. (2017) used a 2-minute rolling mean as a local background, and defined concentrations of either 10 % or 1 standard deviation ppm above that as elevated or peaks. Since our survey approach involved slowing down or stopping the vehicle for several minutes when encountering elevated concentrations, these prolonged measurements of higher concentrations would have influenced a rolling mean. We therefore instead chose to use a symmetric rolling 1st ventile (lowest 5%) over a 15-minute time window calculated separately for both gas analysers. This assumes that the lowest values at any given location will correspond to the background. To test the effect of threshold selection on results obtained we tested three different thresholds: 0.02 ppm (corresponding to 10 × and 52 × the standard deviations of instrument precision above the local background for the UGGA and G2201-*i* analysers, respectively), 0.1 ppm, and 0.3 ppm.
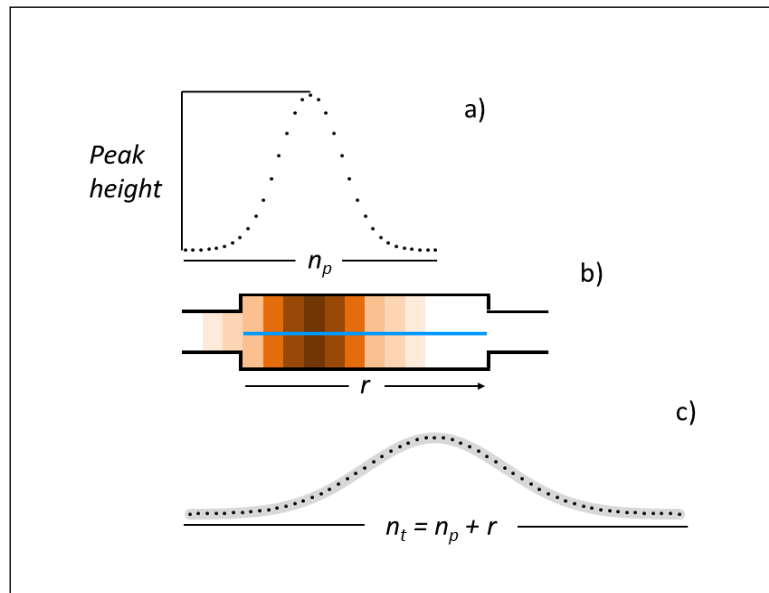
2.6.2. Isotope analysis

To determine the $\delta^{13}CH_4$ isotopic source signatures of emissions, a Miller-Tans plot was created for each peak. In this method, the isotope source signature is given as the slope of a regression of $\delta^{13}C \times [CH_4]$ and $[CH_4]$ (Miller and Tans, 2003). To determine the best fit line for the regression, we used York's method of regression for data with errors in both variables (York, 1969). This method was chosen over more conventional simple linear regression as it provides a more accurate unbiased estimate of the slope (Wehr and Saleska, 2017). The standard error (SE) of the slope was used to evaluate the precision of isotopic measurements. Given that the precision for a single measurement of the G2201-i is 3.01 ‰ (1 σ), numerous measurements at different concentrations are needed to obtain an accurate estimate of $\delta^{13}CH_4$ and so the source signature of smaller peaks cannot be accurately estimated. For this study, we therefore excluded all peaks with a standard error for the regression slope > 5 ‰. This threshold was chosen as it allows distinguishing between microbial sources of CH_4 ($\sim$ -62 ‰) and fossil sources of CH_4 $\sim$ -43 ‰, Schwietzke et al., 2016) with confidence.

2.7. Isotope precision model and sensitivity analysis

2.7.1. Model design

To evaluate the effects of instrument specifications and plume characteristics on the precision of isotope measurements, we programmed a simple physical model to simulate gas measurements in the cavity of a spectroscopic gas analyser. As an exhaustive empirical analysis of the effects of these factors was not feasible, the model acts as a sensitivity analysis to better predict true precisions. The model generates a normally distributed gas peak with a given peak height (maximum concentration above background), isotope signature, and peak length (n_p), which represents the duration for which the peak is measured and therefore determines the number of measurements made (Figure 2). Assuming a measurement frequency of 1 Hz, a peak with n_p = 60 corresponds to passing a peak in 1 min. However, for the sake of general applicability, we defined parameters relative to dimensionless measurement cycles rather than units of volume or time. To account for the dilution of the peak with background air in the cavity, an exchange rate (r) is specified which gives the number of measurement cycles over which the gas in the cavity is completely replaced. For an instrument measuring at 1 Hz, this would correspond to the rise

251   time at which 100 % of the final concentration measurement is reached (T_{100}). This is

252   modelled as a trailing moving average of length r and simulates the measurement of the air

253   mixture in the cavity at any given time point. The total number of measurements per peak,

254   n_t, is thus given as $n_t = n_p + r$. The gas peak is mixed with background air (1.91 ppm CH_4 at -

255   47 ‰ $\delta^{13}C$) by calculating the true CH_4 concentration and $\delta^{13}C$ using a two-pool mixing

256   model for each measurement point. Normal random noise is independently added to the

257   CH_4 concentration and $\delta^{13}C$ with a mean of 0 and a standard deviation representing the

258   instrument precision. Precision is assumed to be concentration independent. These are

259   simplifying assumptions as random noise in concentration and $\delta^{13}C$ of spectroscopic

260   measurements may be correlated (Wehr and Saleska, 2017) and concentration dependent

261   (Rella et al., 2015a).

263   **Figure 3** Graphical representation of isotope precision model, showing a) initial peak with true peak height

264   (maximum concentration above background) and given peak length n_p relative to the number of measurement

265   cycles (represented by points); b) representation of the instrument optical cavity and the gas concentration in

266   it (horizontal blue line represents instrument laser and therefore the cavity length over which concentration is

267   measured); and c) broadened peak as measured by the instrument with random noise added (grey overlay).

268   A York regression is applied to the set of measurements of each peak and the SE of the slope

269   recorded as output. Monte Carlo simulations are run for sets of input parameters (see Table

270   2), performing 1,000 simulations for each combination of instrument precision, peak height,

271   measurement duration (n_p), and instrument exchange rate (r).

272 The model, data processing, and analysis were coded in R version 3.4.3 (R Core Team, 2017),

273 using the IsoplotR (Vermeesch, 2018) and MonteCarlo (Leschinski, 2017) packages. For

274 isotope precision model code, see Takriti (2020).
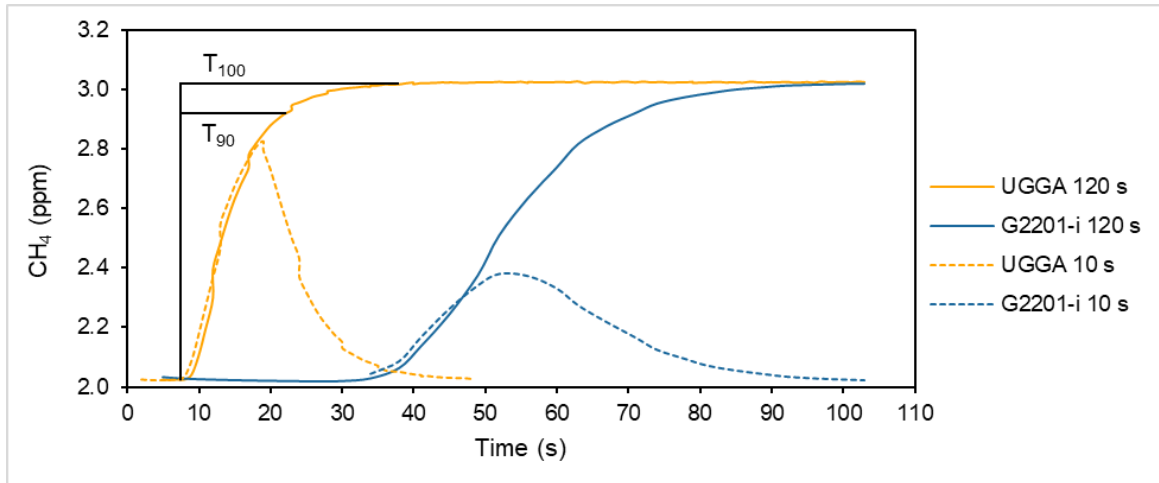
2.7.2. **Model validation**

276 To validate the isotope precision model, we compared model output with SE estimates

277 gathered from the mobile surveys with an SE < 10 ‰. The model was run with instrument

278 precision set to that of our G2201-*i*, and peak height and n_p parameters set to those of

279 observed peaks. The *r* parameter was set to 1 as the measured peaks had already been mixed

280 in the cavity. There was very good agreement between simulated and empirical values with

281 slope = 0.91, R^2 = 0.96 (Figure S 4). The model slightly underestimated SE, likely due to factors

282 such as peak shape or other stochastic processes not considered by the model. For the

283 empirical measurements, SE was proportional to $n^{-0.8}$ (Figure S 5).

3. Results and discussion

3.1. Instrument performance, concentration measurements, and data comparability

3.1.1. Instrument response time

288 When taking real time mobile measurements, where the sampled gas concentrations vary

289 continuously, the rise time of the gas analysers used can affect the measured values. (Figure

290 4). The rise time depends on the cavity volume and the flow rate of the gas analyser. When

291 an analyser is taking in a sample for less than the rise time (or correspondingly the fall time)

292 the final concentration will not be reached. This is shown in Figure 3, where a 3.03 ppm CH_4

293 standard was run through the two instruments in series for either 10 s or 120 s, demonstrating

294 how the instruments differ in transit time, rise time, and peak height. As air in the instrument

295 cavity is continuously replaced, the measured concentration represents a mixture of incoming

296 and present gas, such that the gas peak is broadened inversely proportional to the rate at

297 which the gas is replaced. Hence, both instruments underestimate the true concentration at

298 10 s, but the faster analyser reaches a higher concentration in that timespan. However, the

299 area under the curve of concentration over time is the same for both instruments.
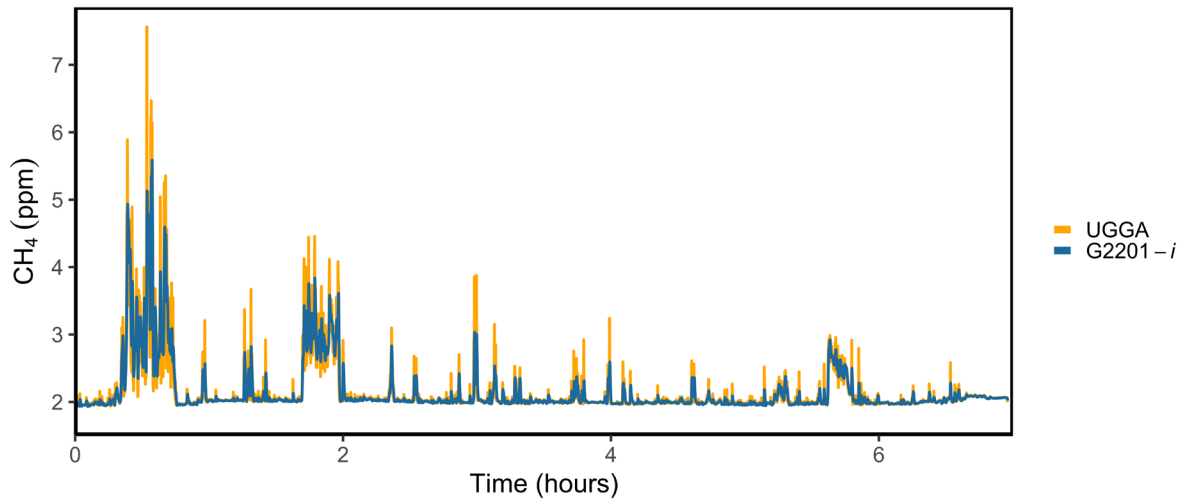
Figure 4 Concentration of a 3.03 ppm CH_4 standard gas as measured on a G2201-*i* isotopic gas analyser and a UGGA connected in series. Solid lines show measurements where the standard gas was connected for 120 s and both instruments reached stable readings. Dashed lines show measurements where the standard gas was connected for 10 s. Horizontal lines indicate rise times at which 90% (T_{90}) or 100% (T_{100}) of the final concentration have been reached for the UGGA.
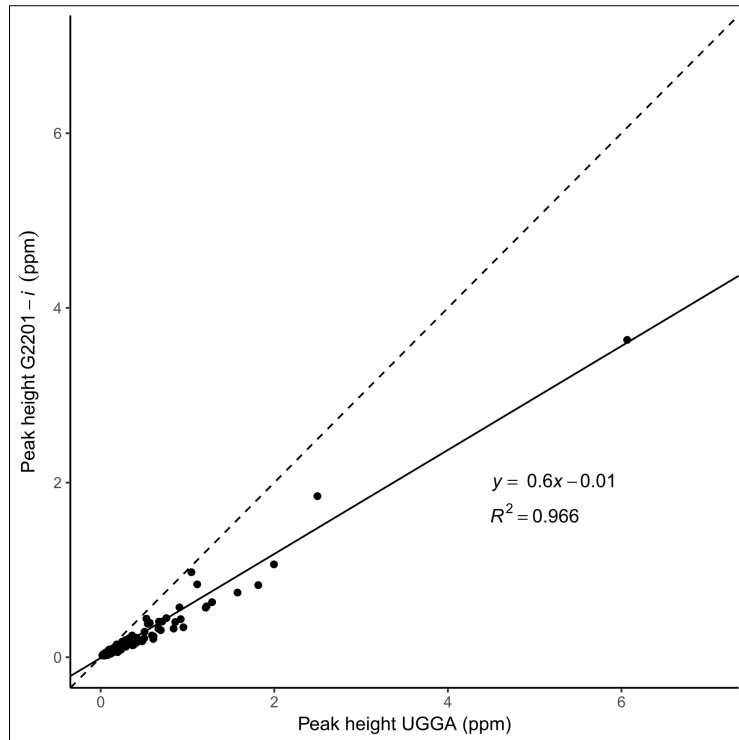
3.1.2. **Methane concentrations**

To assess the effect of differing rise times under real world conditions, we compared CH_4 concentration measurements of the UGGA and G2201-*i* gas analysers from four sampling days. There was a consistent discrepancy in measured CH_4 concentration between the two gas analysers, with the G2201-*i* reporting lower concentrations (Figure 5). We plotted maximum peak concentrations measured by the two instruments against each other and found values from the G2201-*i* to be 40 % lower compared to the UGGA (Figure 6). This is a relative measurement, as the true peak concentrations are not known. The relationship between the peak concentrations of the two instruments was fairly stable throughout the surveys, and there was only a very weak positive relationship between the ratio of the G2201-*i* and UGGA peak heights and the driving speed (R^2 = 0.02, F(1, 224), p = 0.034). Therefore, differences in peak concentrations were still observed during stationary measurements, as demonstrated in Figure S 1, which shows concentration data collected over a ten-minute period in a parking lot close to a gas leak If sampled CH_4 concentrations are not constant, either due to micrometeorological variation or a moving sampling system, instruments may not report true concentrations unless their response was instantaneous. Such dependence of concentration measurements on rise time may lead to underestimating emissions during

323 mobile surveys, and limits the comparability of results, particularly when comparing data

324 between instruments with significantly different rise times.

326 **Figure 5** Mobile CH$_4$ measurements made simultaneously by a G2201-*i* isotopic gas analyser and a UGGA

327 greenhouse gas analyser connected in series during mobile surveys. Only data points above background

328 concentration for at least one of the analysers are shown.

329

Figure 6 Maximum peak concentration above background for CH_4 peaks measured either by a G2201-i or a UGGA (n = 228). Peaks recorded by both analysers were matched if they overlapped temporally. In case of multiple overlapping peaks, the highest peak was selected. Dashed line shows slope = 1.

3.1.3. **Rise time correction**

To explore the potential for mathematical correction of rise times we adapted a correction algorithm based on a second order differential equation from Wong et al. (1998), developed by Arieli and Van Liew (1981), and applied it to standard gas measurements on our two instruments (see SI). For a step change in concentration, the algorithm reduced the effective rise time (T_{90}) by 42 % to 22 s for the G2201-i and 29 % to 10 s for the UGGA and reduced the associated underestimation in CH_4 concentrations (Figure S 3, Table S 1). While amplifying noise in the measurements along with the signal, such methods may provide concentration values that are closer to true peak plume concentrations for mobile measurements.

3.1.4. **Peak count**

Another way to characterise emissions sources is to count the number of peaks, i.e. concentrations that exceed some threshold, encountered during mobile surveys of specific regions (Boothroyd et al., 2016). However, this measure is also dependent on instrument response time, as any given threshold will be reached more quickly and therefore more
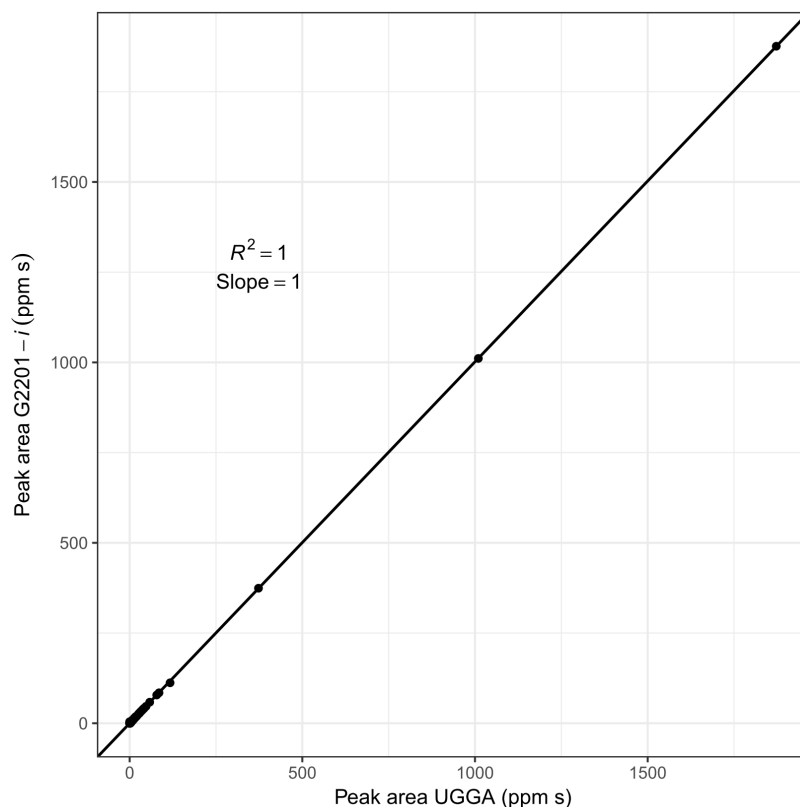
348　frequently on a faster instrument. Table 1 shows the number of CH_4 peaks above background

349　levels for both instruments at three different thresholds. Depending on the selected

350　threshold, around 60 % fewer peaks were detected on the G2201-*i* compared to the UGGA,

351　due to the difference in response time. Selecting a higher threshold will mainly remove small

352　and locally constrained emission plumes from the analysis but higher thresholds also

353　eliminated peaks whose isotopic signature could be determined with sufficient precision, thus

354　potentially eliminating useful data.

355　**Table 1** Number of CH_4 peaks counted during mobile surveys at different thresholds with two gas analysers

356　and the number of peaks whose $\delta^{13}CH_4$ signature could be estimated with a precision (SE) of < 5 ‰.

Threshold (ppm)	G2201-*i*	UGGA	G2201-*i*/UGGA	SE < 5 ‰
0.02	236	726	0.33	6
0.1	67	157	0.43	4
0.3	32	80	0.40	3

357　3.1.5.　**Peak area**

358　While peaks measured by a slower instrument are broadened relative to those measured by

359　a faster instrument, the peak area remains the same (Figure 3). When comparing peak areas

360　obtained from mobile surveys, the UGGA would occasionally measure several distinct peaks

361　for every one peak of the G2201-*i*. We accounted for this by adding temporally overlapping

362　peak areas together. This resulted in a perfect relationship between the instruments,

363　indicating that peak areas provide a robust means of comparing data between instruments

364　(Figure 6). Peak areas will be sensitive to driving speeds as the measurement duration and

365　therefore area increases with decreasing speed. However, since driving speed is known and

366　peak area decreases linearly with speed, this can be corrected for (Figure S 2). Also, depending

367　on the research question, peak areas may provide additional insight. For example, Fischer et

368　al. (2017) found that peak areas are correlated with emission rate for urban gas pipeline leaks.

369　Such relationships may exist for other sources and peak areas may thus aide quantification of

370　emission rates.

Figure 7 Scatter plot of peak CH_4 areas (n = 230) measured across four mobile surveys as measured by a G2201-i isotopic gas analyser and a UGGA greenhouse gas analyser connected in series.

3.2. Isotope precision model and sensitivity analysis

For mobile isotopic measurements, the isotopic signature is determined through regression analysis. The effective precision of the measurements therefore depends not only on the precision of the instrument and measurement duration, but also on factors such as the range of concentrations measured and the instrument response time. As exploring the relative importance of these effects experimentally is technically challenging, we programmed a physical model simulating gas flow through a spectroscopic analyser and used a Monte Carlo simulation to generate stochastic noise in the measurements, simulating random error.

We ran the model with all possible combinations of parameters, namely instrument precision, peak height above background, measurement duration (n_p), and instrument exchange rate (r). For isotopic precision, we used settings approximating the performance of our G2201-*i*, as well as settings of hypothetical instruments with higher precision. For the CH_4 plume parameters, we used a range of values representative of data collected during our surveys or those reported in the literature.

388 As would be expected, the precision of plume measurements increases linearly with the
389 isotopic precision of the analyser (Table 2). Both isotopic and concentration measurement
390 precision influence the precision estimate of plume isotope measurements. However, since
391 the precision of concentration measurements of current spectroscopic CH_4 analysers is
392 around four orders of magnitude higher than the precision of isotopic measurements,
393 improving concentration precision has negligible effects (data not shown), and was therefore
394 kept constant for all model iterations.

395 Peak height, i.e. the maximum concentration of the plume above background, also had a
396 strong effect on isotopic precision as it extends the range of both variables in the Miller-Tans
397 regression model. Because isotopic precision of gas analysers may increase with
398 concentration, our model may slightly underestimate the improvement in precision.
399 Increasing n_p (i.e. increasing measurement duration) also decreases SE, such that SE is
400 minimised by increasing both peak height and n_p. The relationship between SE and peak
401 height and SE and n_p are both described by power functions (Figure S 6 & Figure S 7), meaning
402 that for the practical domains, initial improvements in either of these parameters will lead to
403 large improvements in isotopic precision. However, approaching the asymptote any further
404 will only result in marginal precision improvements. For practical applications, it may
405 therefore not be possible to fully compensate for low plume concentrations by increasing the
406 measurement time, e.g. by taking stationary downwind measurements. Increasing r, i.e. the
407 rise time of the instrument, increases n_t, and therefore the number of measurements per
408 peak, but it also increases response time and effectively reduces the measured maximum
409 concentration. As outlined above, this may have a significant effect on SE depending on the
410 values of n_p and the initial peak height. Such trade-offs occur e.g. when using AirCore
411 technology where sampled gas is captured in a narrow tube during mobile surveys, and then
412 "replayed" at a slower speed to increase the precision of the isotopic measurements (Karion
413 et al., 2010; Rella et al., 2015b).

414 Overall, our model demonstrates that for a given set of instrument parameters, achieved
415 isotopic precision will heavily depend on both plume concentration and measurement
416 duration. For example, increasing concentration from 1 ppm CH_4 to 2.5 ppm CH_4 above
417 background while increasing n_p from 100 to 250 (corresponding to an increase from ~6.5 min
418 to ~16 min at 0.26 Hz) reduces uncertainty more than threefold (Table 2).

419 **Table 2** Results of Monte Carlo simulations of the effects of instrument and plume parameters on the precision

420 of simulated $\delta^{13}CH_4$ plume measurements. Parameters: precision is instrument precision given as 1σ for a

421 single isotopic measurement, r is number of measurement cycles over which gas in the instrument cavity is

422 replaced, n_p is measurement cycles, peak height is max peak concentration above background. Simulations of

423 plume measurements for each parameter combination were repeated 1000 times. Precision of $\delta^{13}CH_4$

424 measurements is calculated as mean standard error for the slope of a Miller-Tans plot using York regression.

Precision (‰)	r	n_p	Peak height (ppm)							
			0.5	1	2.5	5	7.5	10	15	20
3.0	20	100	3.81	2.13	1.13	0.78	0.66	0.60	0.53	0.50
		250	2.35	1.33	0.71	0.50	0.42	0.39	0.35	0.32
		500	1.66	0.94	0.50	0.35	0.30	0.27	0.25	0.23
		1000	1.18	0.67	0.36	0.25	0.21	0.19	0.17	0.16
	40	100	4.26	2.33	1.17	0.78	0.65	0.58	0.51	0.47
		250	2.37	1.33	0.71	0.49	0.42	0.38	0.34	0.32
		500	1.66	0.94	0.50	0.35	0.30	0.27	0.24	0.23
		1000	1.18	0.66	0.36	0.25	0.21	0.19	0.17	0.16
	60	100	4.91	2.62	1.25	0.80	0.64	0.56	0.49	0.44
		250	2.44	1.36	0.71	0.49	0.42	0.38	0.33	0.31
		500	1.66	0.94	0.50	0.35	0.30	0.27	0.24	0.23
		1000	1.17	0.66	0.35	0.25	0.21	0.19	0.17	0.16
1.5	20	100	1.90	1.06	0.56	0.39	0.33	0.30	0.27	0.25
		250	1.17	0.66	0.35	0.25	0.21	0.19	0.17	0.16
		500	0.83	0.47	0.25	0.18	0.15	0.14	0.12	0.11
		1000	0.59	0.33	0.18	0.13	0.11	0.10	0.09	0.08
	40	100	2.12	1.16	0.58	0.39	0.32	0.29	0.25	0.23
		250	1.18	0.67	0.35	0.25	0.21	0.19	0.17	0.16
		500	0.83	0.47	0.25	0.18	0.15	0.14	0.12	0.11
		1000	0.59	0.33	0.18	0.12	0.11	0.10	0.09	0.08
	60	100	2.45	1.31	0.63	0.40	0.32	0.28	0.24	0.22
		250	1.22	0.68	0.36	0.25	0.21	0.19	0.17	0.16
		500	0.83	0.47	0.25	0.17	0.15	0.14	0.12	0.11
		1000	0.58	0.33	0.18	0.12	0.11	0.10	0.09	0.08
0.5	20	100	0.63	0.35	0.19	0.13	0.11	0.10	0.09	0.08
		250	0.39	0.22	0.12	0.08	0.07	0.06	0.06	0.05
		500	0.27	0.15	0.08	0.06	0.05	0.05	0.04	0.04
		1000	0.19	0.11	0.06	0.04	0.04	0.03	0.03	0.03
	40	100	0.70	0.38	0.19	0.13	0.11	0.10	0.08	0.08
		250	0.39	0.22	0.12	0.08	0.07	0.06	0.06	0.05
		500	0.27	0.15	0.08	0.06	0.05	0.05	0.04	0.04
		1000	0.19	0.11	0.06	0.04	0.04	0.03	0.03	0.03
	60	100	0.81	0.43	0.21	0.13	0.11	0.09	0.08	0.07
		250	0.40	0.22	0.12	0.08	0.07	0.06	0.06	0.05
		500	0.27	0.15	0.08	0.06	0.05	0.04	0.04	0.04
		1000	0.19	0.11	0.06	0.04	0.04	0.03	0.03	0.03

425

4. Conclusions

It is important to consider how instrument setup and sampling conditions can affect the results of mobile measurements. We show that slower instrument response time can lead to a significant underestimation of mobile concentration measurements. This should be taken into account when comparing absolute values across different setups, and we therefore recommend consistently reporting instrument rise time for mobile applications. While mathematical corrections may improve concentration estimates, our results demonstrate that peak areas of emission plumes are independent of instrument response times and provide an alternative and more robust means to compare data obtained between different instrument setups. Additionally, we show that isotopic precision of mobile measurements determined with regression methods is not just a function of instrument precision, but also instrument speed, measurement duration and, importantly, concentration range. The model we developed can predict these effects on isotopic precision for any given instrumental setup and application. It can therefore inform choices on equipment used, as well as sampling strategies, and estimate expected uncertainty. As the underlying principles are independent of chemical species, our findings are relevant to applications other than CH_4 measurements, such as mobile air pollution measurements (Apte et al., 2017) or the emerging field of unmanned aerial vehicle based measurement systems.

6. References

Albertson, J.D., Harvey, T., Foderaro, G., Zhu, P., Zhou, X., Ferrari, S., Amin, M.S., Modrak, M., Brantley, H., Thoma, E.D., 2016. A Mobile Sensing Approach for Regional Surveillance of Fugitive Methane Emissions in Oil and Gas Production. Environ. Sci. Technol. 50, 2487–2497. https://doi.org/10.1021/acs.est.5b05059

Allen, G., Hollingsworth, P., Kabbabe, K., Pitt, J.R., Mead, M.I., Illingworth, S., Roberts, G., Bourn, M., Shallcross, D.E., Percival, C.J., 2019. The development and trial of an unmanned aerial system for the measurement of methane flux from landfill and greenhouse gas emission hotspots. Waste Manag. 87, 883–892. https://doi.org/10.1016/j.wasman.2017.12.024

Apte, J.S., Messier, K.P., Gani, S., Brauer, M., Kirchstetter, T.W., Lunden, M.M., Marshall, J.D., Portier, C.J., Vermeulen, R.C.H., Hamburg, S.P., 2017. High-Resolution Air Pollution Mapping with Google Street View Cars: Exploiting Big Data. Environ. Sci. Technol. 51, 6999–7008. https://doi.org/10.1021/acs.est.7b00891

Arieli, R., Van Liew, H.D., 1981. Corrections for the response time and delay of mass spectrometers. J. Appl. Physiol. 51, 1417–1422.

Boothroyd, I.M., Almond, S., Worrall, F., Davies, R.J., 2016. Assessing the fugitive emission of CH_4 via migration along fault zones – Comparing potential shale gas basins to non-shale basins in the UK. Sci. Total Environ. https://doi.org/10.1016/j.scitotenv.2016.09.052

Brunner, J.X., Westenskow, D.R., 1988. How the rise time of carbon dioxide analysers influences the accuracy of carbon dioxide measurements. Br. J. Anaesth. 61, 628–638. https://doi.org/10.1093/bja/61.5.628

Czepiel, P.M., Mosher, B., Harriss, R.C., Shorter, J.H., McManus, J.B., Kolb, C.E., Allwine, E., Lamb, B.K., 1996. Landfill methane emissions measured by enclosure and atmospheric tracer methods. J. Geophys. Res. 101, 16711. https://doi.org/10.1029/96JD00864

Eapi, G.R., Sabnis, M.S., Sattler, M.L., 2014. Mobile measurement of methane and hydrogen sulfide at natural gas production site fence lines in the Texas Barnett Shale. J. Air Waste Manage. Assoc. 64, 927–944. https://doi.org/10.1080/10962247.2014.907098

Etminan, M., Myhre, G., Highwood, E.J., Shine, K.P., 2016. Radiative forcing of carbon dioxide, methane, and nitrous oxide: A significant revision of the methane radiative forcing. Geophys. Res. Lett. 43, 12,614-12,623. https://doi.org/10.1002/2016GL071930

Farmery, A.D., Hahn, C.E., 2000. Response-time enhancement of a clinical gas analyzer facilitates measurement of breath-by-breath gas exchange. J. Appl. Physiol. 89, 581–589.

Fischer, J.C. von, Cooley, D., Chamberlain, S., Gaylord, A., Griebenow, C.J., Hamburg, S.P., Salo, J., Schumacher, R., Theobald, D., Ham, J., 2017. Rapid, Vehicle-Based Identification of Location and Magnitude of Urban Natural Gas Pipeline Leaks. Environ. Sci. Technol. 51, 4091–4099. https://doi.org/10.1021/acs.est.6b06095

489 Jackson, R.B., Down, A., Phillips, N.G., Ackley, R.C., Cook, C.W., Plata, D.L., Zhao, K., Philips,
490   N.G., Ackley, R.C., Cook, C.W., Plata, D.L., Zhao, K., 2014. Natural gas pipeline leaks across
491   Washington, DC. Environ. Sci. Technol. 48, 2051–8. https://doi.org/10.1021/es404474x

492 Karion, A., Sweeney, C., Tans, P., Newberger, T., 2010. AirCore: An Innovative Atmospheric
493   Sampling   System.   J.   Atmos.   Ocean.   Technol.   27,   1839–1853.
494   https://doi.org/10.1175/2010JTECHA1448.1

495 Leschinski, C.H., 2017. MonteCarlo: Automatic Parallelized Monte Carlo Simulations.

496 Liu, S., Yang, X., Zhou, X., 2020. Development of a low-cost UAV-based system for CH 4
497   monitoring   over   oil   fields.   Environ.   Technol.   0,   1–10.
498   https://doi.org/10.1080/09593330.2020.1724199

499 Lopez, M., Sherwood, O.A., Dlugokencky, E.J., Kessler, R., Giroux, L., Worthy, D.E.J., 2017.
500   Isotopic signatures of anthropogenic CH4 sources in Alberta, Canada. Atmos. Environ.
501   164, 280–288. https://doi.org/10.1016/j.atmosenv.2017.06.021

502 Miller, J.B., Tans, P.P., 2003. Calculating isotopic fractionation from atmospheric
503   measurements at various scales. Tellus, Ser. B Chem. Phys. Meteorol. 55, 207–214.
504   https://doi.org/10.1034/j.1600-0889.2003.00020.x

505 Mønster, J.G., Samuelsson, J., Kjeldsen, P., Rella, C.W., Scheutz, C., 2014. Quantifying methane
506   emission from fugitive sources by combining tracer release and downwind
507   measurements - a sensitivity analysis based on multiple field surveys. Waste Manag. 34,
508   1416–28. https://doi.org/10.1016/j.wasman.2014.03.025

509 R Core Team, 2017. R: A Language and Environment for Statistical Computing.

510 Rella, C.W., Hoffnagle, J., He, Y., Tajima, S., 2015a. Local- and regional-scale measurements of
511   CH_4, $\delta^{13}CH_4$, and C_2H_6 in the Uintah Basin using a mobile stable isotope analyzer. Atmos.
512   Meas. Tech. 8, 4539–4559. https://doi.org/10.5194/amt-8-4539-2015

513 Rella, C.W., Hoffnagle, J., He, Y., Tajima, S., 2015b. Local- and regional-scale measurements of
514   CH4, Δ13CH4, and C2H6 in the Uintah Basin using a mobile stable isotope analyzer.
515   Atmos. Meas. Tech. 8, 4539–4559. https://doi.org/10.5194/amt-8-4539-2015

516 Schena, J., Thompson, J., Crone, R.K., 1984. Mechanical influences on the capnogram. Crit.
517   Care Med. 12, 672–674. https://doi.org/10.1097/00003246-198408000-00015

518 Schwietzke, S., Sherwood, O.A., Bruhwiler, L.M.P., Miller, J.B., Etiope, G., Dlugokencky, E.J.,
519   Michel, S.E., Arling, V.A., Vaughn, B.H., White, J.W.C., Tans, P.P., 2016. Upward revision
520   of global fossil fuel methane emissions based on isotope database. Nature 538, 88–91.
521   https://doi.org/10.1038/nature19797

522 Takriti, M., 2020. Isotope precision model. https://doi.org/10.5281/zenodo.3748490

523 Tang, Y., Turner, M.J., Baker, A.B., 2005. Effects of lung time constant, gas analyser delay and
524   rise time on measurements of respiratory dead-space. Physiol. Meas. 26, 1103–1114.

https://doi.org/10.1088/0967-3334/26/6/019

Turner, A.J., Jacob, D.J., Benmergui, J., Wofsy, S.C., Maasakkers, J.D., Butz, A., Hasekamp, O., Biraud, S.C., 2016. A large increase in U.S. methane emissions over the past decade inferred from satellite data and surface observations. Geophys. Res. Lett. 43, 2218–2224. https://doi.org/10.1002/2016GL067987

Vermeesch, P., 2018. IsoplotR: A free and open toolbox for geochronology. Geosci. Front. https://doi.org/10.1016/j.gsf.2018.04.001

Wehr, R., Saleska, S.R., 2017. The long-solved problem of the best-fit straight line: application to isotopic mixing lines. Biogeosciences 14, 17–29. https://doi.org/10.5194/bg-14-17-2017

Williams, E., 2011. Aviation Formulary v1.46 [WWW Document]. URL http://www.edwilliams.org/avform.htm (accessed 5.11.18).

Wong, L., Hamilton, R., Palayiwa, E., Hahn, C., 1998. A real time algorithm to improve the response time of a clinical multigas analyser. Algorythm 14, 441–446. https://doi.org/10.1023/A:1009941900141

York, D., 1969. Least squares fitting of a straight line with correlated errors. Earth Planet. Sci. Lett. 5, 320–324. https://doi.org/10.1016/S0012-821X(68)80059-7

Yoshida, H., Mønster, J.G., Scheutz, C., 2014. Plant-integrated measurement of greenhouse gas emissions from a municipal wastewater treatment plant. Water Res. 61, 108–18. https://doi.org/10.1016/j.watres.2014.05.014

Zazzeri, G., Lowry, D., Fisher, R.E., France, J.L., Lanoisellé, M., Nisbet, E.G., 2015. Plume mapping and isotopic characterisation of anthropogenic methane sources. Atmos. Environ. 110, 151–162. https://doi.org/10.1016/j.atmosenv.2015.03.029